

## RESEARCH ARTICLE

View Article Online  
View Journal | View IssueCite this: *Org. Chem. Front.*, 2024, **11**, 1420

## Formation of ylidenehydrazines enabled by manganese-catalyzed acceptorless dehydrogenative coupling†

Fangchao Wang,<sup>‡</sup> Ding Ding,<sup>‡</sup> Chunyan Zhang \*<sup>a</sup> and Guoying Zhang \*<sup>b,c</sup>

Catalytic dehydrogenation, which exhibits highly atom-economical and chemo-selective properties, converts multiple green sustainable alcohols to critical molecules and is a highly desirable and elusive process; furthermore, the dehydrogenation of alcohols with hydrazines produces ylidenehydrazines, which are versatile building blocks in the formation of numerous pharmaceuticals. However, the syntheses of functionalized ylidenehydrazines involve multi-step reactions that require harsh conditions. Herein, we report a practical one-pot catalytic tandem dehydrogenative condensation coupling of hydrazines with alcohols and halides to form ylidenehydrazines *via* an acceptorless dehydrogenative coupling strategy, overcoming the challenge of selectivity in multicomponent reactions. The system is based on the Earth-abundant metal Mn, which is stabilized by a novel bench-stable PNN pincer ligand derived from aminoindazole. A large series of functionalized ylidenehydrazines is obtained in high yields with excellent selectivities, and gram-scale ylidenehydrazines are prepared using this protocol. Notably, using this protocol, several pharmaceuticals may be easily synthesized in a one-pot manner. This strategy significantly broadens the scope of Mn-catalyzed dehydrogenative condensation coupling for synthesizing unsaturated molecules.

Received 13th November 2023,  
Accepted 6th January 2024

DOI: 10.1039/d3qo01890c

rsc.li/frontiers-organic

## Introduction

Ylidenehydrazines, which exhibit remarkable biological activities, are frequently used in pharmaceuticals, agrochemicals, and functional materials (Fig. 1A).<sup>1</sup> They also serve as attractive precursors in a series of transformations that form various complex, functional compounds.<sup>2</sup> Owing to their scientific applications, considerable effort has been devoted to synthesizing these privileged scaffolds, particularly *via* metal-catalyzed dehydrogenative condensation and/or nucleophilic substitution strategies.<sup>3</sup> However, most approaches require super stoichiometric amounts of external additives or harsh reaction conditions, particularly multi-step reactions, which undeniably result in decreased atom efficiency owing to complex operation processes and the formation of undesired waste byproducts

(Fig. 1D).<sup>4</sup> Therefore, a novel and direct method is required for one-pot synthesis of hydrazones using bulk raw materials.

The efficient and highly selective conversion of alcohols to significant compounds is highly attractive because alcohols may be obtained from abundant lignocellulose biomass, which may reduce CO<sub>2</sub> emissions and conserve finite fossil carbon resources.<sup>5</sup> An atom economical dehydrogenative reaction is a green method of transforming alcohols to produce H<sub>2</sub> or H<sub>2</sub>O byproducts.<sup>6</sup> Dehydrogenative transformations have been successfully developed over the past decades.<sup>7</sup> Early catalytic dehydrogenation reactions were mostly based on the use of rare noble metals (Ir, Pt, Rh, and Ru) as catalysts (Fig. 1B).<sup>8</sup> Recently, the use of abundant 3d metals (Fe, Co, and Ni) as efficient catalysts in these transformations has emerged.<sup>9</sup> Mn metal catalytic systems have also been developed for use in catalytic dehydrogenative transformations, displaying novel patterns of selectivity compared to those of rare noble metals.<sup>10</sup> Additionally, the sustainable generation of H<sub>2</sub> *via* dehydrogenation is highly attractive because of its central role as an energy carrier and reducing agent. Therefore, novel reactions mediated by 3d metal catalysts that transform green or sustainable starting materials into significant classes of complex molecules *via* the dehydrogenation of alcohols and H<sub>2</sub> generation are highly desirable.

To the best of our knowledge, transition metal catalyzed dehydrogenative transformation of alcohols with hydrazines

<sup>a</sup>College of Ecology, Taiyuan University of Technology, Taiyuan 030001, China.  
E-mail: zhangchunyan@tyut.edu.cn

<sup>b</sup>State Key Laboratory of Coal Conversion, Institute of Coal Chemistry, Chinese Academy of Sciences, Taiyuan 030001, China

<sup>c</sup>University of Chinese Academy of Sciences, Beijing 100049, China.  
E-mail: zhanggy@sxicc.ac.cn

†Electronic supplementary information (ESI) available. CCDC 2288831 and 2288839. For ESI and crystallographic data in CIF or other electronic format see DOI: <https://doi.org/10.1039/d3qo01890c>

‡These authors contributed equally to this work.



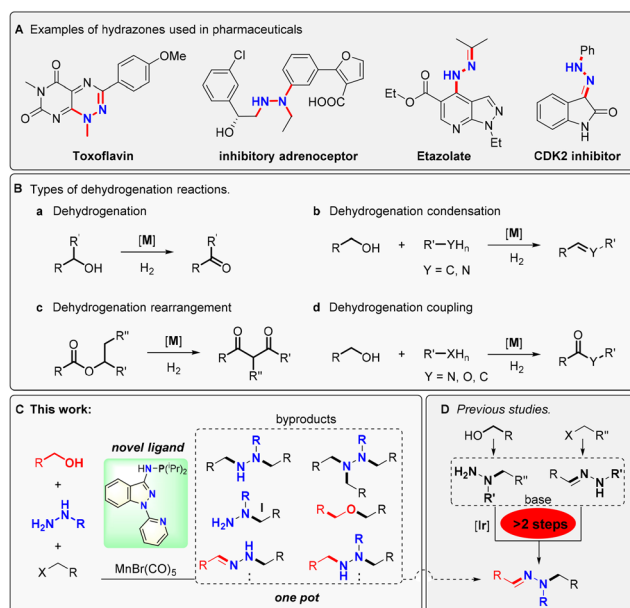


**Fig. 1** Current state of the field of hydrazones and the synthesis described herein. (A) Examples of hydrazones used in pharmaceuticals. (B) Types of dehydrogenation reactions. (C) This work. (D) Previous studies.

and halides remains unexplored. The evident challenge of this reaction is that the accelerator or catalyst is surrounded by a large excess of active substrates under the reaction conditions, and thus, undesired byproducts are easily generated. To overcome this challenge, improving the affinity between intermediate **I** (*in situ*-formed hydrazine with halides) and the aldehyde species (*in situ* dehydrogenation of the alcohol) is critical. Additionally, ensuring that (i) intermediate **I** is sufficiently stable in the reactive system and (ii) both dehydrogenation of the alcohol and condensation with **I** occur *via* similar rapid processes such that the formation of byproducts is largely suppressed is crucial. In this study, we report an efficient catalytic system that combines the Earth-abundant Mn metal with a readily available PN<sub>3</sub>N pincer ligand. The catalytic system exhibits an unprecedented, practical catalytic condensation coupling of hydrazines with alcohols and halides to form ylidenhydrazines *via* an acceptorless dihydrogen coupling strategy; the challenge of selectivity in a one-pot multicomponent reaction is thus overcome (Fig. 1C).

Furthermore, dehydrogenative condensation cross-coupling reactions may add to the existing synthesis concepts used in generating H<sub>2</sub> in chemical reactions, such as alcohol dehydrogenation,<sup>11</sup> dehydrogenative condensation,<sup>12</sup> rearrangement,<sup>13</sup> and coupling reactions (Fig. 1B).<sup>14</sup>

## Results and discussion

Based on our experience with Mn-promoted dehydrogenative coupling reactions,<sup>15</sup> phenyl methanol (**A1**), phenylhydrazine (**B1**), and (bromomethyl)benzene (**C1**) were used as model sub-

strates, and dehydrogenative condensation was performed in the presence of Mn(CO)<sub>5</sub>Br with bi- or tridentate ligands (Table 1). The desired product was obtained in a trace amount using a P-N-based accessory ligand (**L1**), and the reaction efficiency was improved when using **L2** as a ligand (entries 1 and 2). The use of other tridentate ligands (**L3–L5**) functionalized on the pyridyl moiety did not improve the reactivity under similar reaction conditions (entries 3–5). Similar results were obtained using other P-N-N (**L6–L9**)-based ligands with different indazole phenyl groups, indicating that the conversion is insensitive to the electrical properties of the indazole backbone (entries 6–9). Evaluation of the P-N-N ligands with different phosphine groups on the amine of the indazole revealed that the conversion is sensitive to the electrostatic and steric hindrance of the ligand, with **L10–L11** providing optimal regioselectivity toward the condensation product. **L11** is the most effective, affording the desired **D1** in 91% yield and with excellent selectivity (**E1**, 1,2-dibenzyl-1-phenylhydrazine). **D1** is obtained in 96% yield after a prolonged reaction time, and only a trace amount of the desired product is obtained in the absence of the Mn catalyst or ligand. Furthermore, the desired product **D1** is not obtained when MnBr<sub>2</sub> is stabilized using **L11** (entry 14). The optimal results in terms of the hydrazone adducts are obtained after the final optimization of the reaction parameters, with **L11** being the most active ligand (ESI†).<sup>16</sup>

**Table 1** Optimization of reaction conditions

Entry	Pre-catalyst	Ligand	<b>D1</b> <sup>a</sup> (%)	<b>D1</b> : <b>E1</b> <sup>a</sup>
1	Mn(CO) <sub>5</sub> Br	<b>L1</b>	<5	8 : 1
2	Mn(CO) <sub>5</sub> Br	<b>L2</b>	62 (66) <sup>b</sup>	>20 : 1
3	Mn(CO) <sub>5</sub> Br	<b>L3</b>	41	>20 : 1
4	Mn(CO) <sub>5</sub> Br	<b>L4</b>	54	18 : 1
5	Mn(CO) <sub>5</sub> Br	<b>L5</b>	22	19 : 1
6	Mn(CO) <sub>5</sub> Br	<b>L6</b>	60	18 : 1
7	Mn(CO) <sub>5</sub> Br	<b>L7</b>	63	18 : 1
8	Mn(CO) <sub>5</sub> Br	<b>L8</b>	51	17 : 1
9	Mn(CO) <sub>5</sub> Br	<b>L9</b>	47	18 : 1
10	Mn(CO) <sub>5</sub> Br	<b>L10</b>	82 (85) <sup>b</sup>	19 : 1
11	Mn(CO) <sub>5</sub> Br	<b>L11</b>	91 (96) <sup>b</sup>	>20 : 1
12	Mn(CO) <sub>5</sub> Br	—	0	—
13	—	<b>L11</b>	0	—
14	MnB <sub>2</sub>	<b>L11</b>	0	—

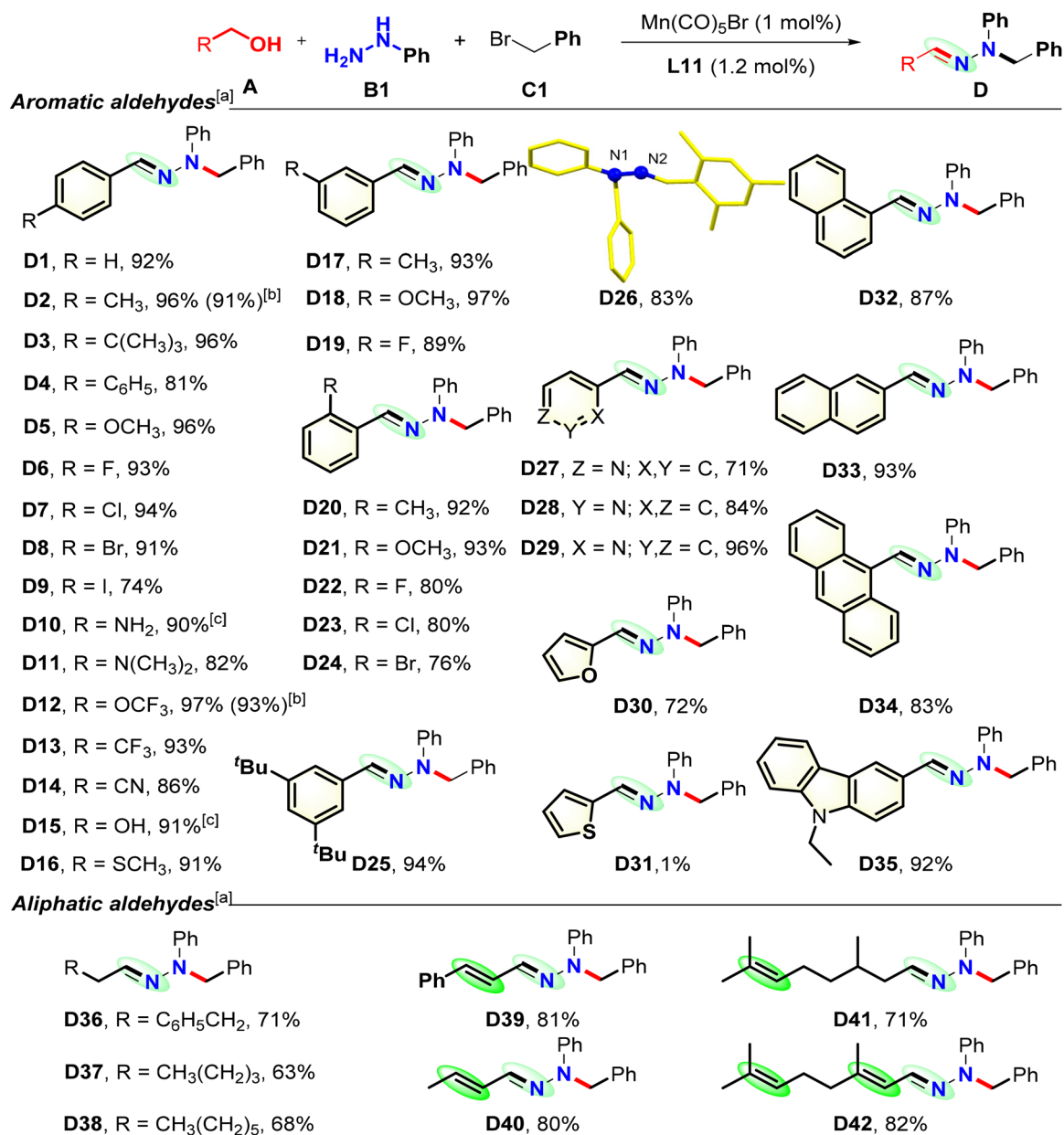
**L1**: X = C, R<sup>1</sup> = H  
**L2**: X = N, R<sup>1</sup> = H  
**L3**: X = N, R<sup>1</sup> = 3-Cl  
**L4**: X = N, R<sup>1</sup> = 4-Cl  
**L5**: X = N, R<sup>1</sup> = 4-Cl  
**L6**: R<sup>2</sup> = 4-CH<sub>3</sub>  
**L7**: R<sup>2</sup> = 6-CH<sub>3</sub>  
**L8**: R<sup>2</sup> = 4-Cl  
**L9**: R<sup>2</sup> = 4-CF<sub>3</sub>  
**L10**: PCy<sub>2</sub>  
**L11**: P<sup>t</sup>Pr<sub>2</sub>

<sup>a</sup> Conditions: **A1** (0.8 mmol), **B1** (0.5 mmol), **C1** (0.7 mmol), Mn(CO)<sub>5</sub>Br (1.0 mol%), **L1–L11** (1.2 mol%), <sup>t</sup>BuOK (1.0 mmol), THF (3.0 mL), 100 °C, 6 h. The yields of **D1** were determined *via* GC using *n*-cetane as the internal standard. <sup>b</sup> 12 h.



The generality and limitations of the dehydrogenative condensation were investigated. Initially, **C1** and **B1** were used as model reagents with various primary alcohols (Scheme 1). Fortunately, benzyl alcohols bearing electron-donating and -withdrawing groups are tolerated well under the reaction conditions, affording the desired corresponding products in high to excellent yields (**D1–D16**). The electronic properties of the phenyl rings in the benzyl alcohols do not affect the reaction. Critically, benzyl alcohols with various substituents at their *ortho*-positions are transformed smoothly under the standard conditions, but hindrance at the phenyl ring affects the transformation efficiencies (**D20–D24**). The dehydrogenative trans-

formations with halo-substituted alcohols proceed smoothly to generate the corresponding desired hydrazones in 74–94% yields (**D6–D9**, **D22–D24**), thus enabling further possible complex transformations, such as metal catalyzed carbonylation or cross-coupling reactions. Notably, the use of an alcohol with a free amino or hydroxyl moiety on the phenyl group, respectively, produces **D10** or **D15** in a high yield. Amino, trifluoromethoxy, trifluoromethyl, and cyano groups tolerate this conversion, and their corresponding products are obtained in high yields. Meanwhile, heterocyclic moieties, including pyridine, furan, and thiofuran, may be smoothly incorporated into the hydrazone molecules using the corresponding alcohols



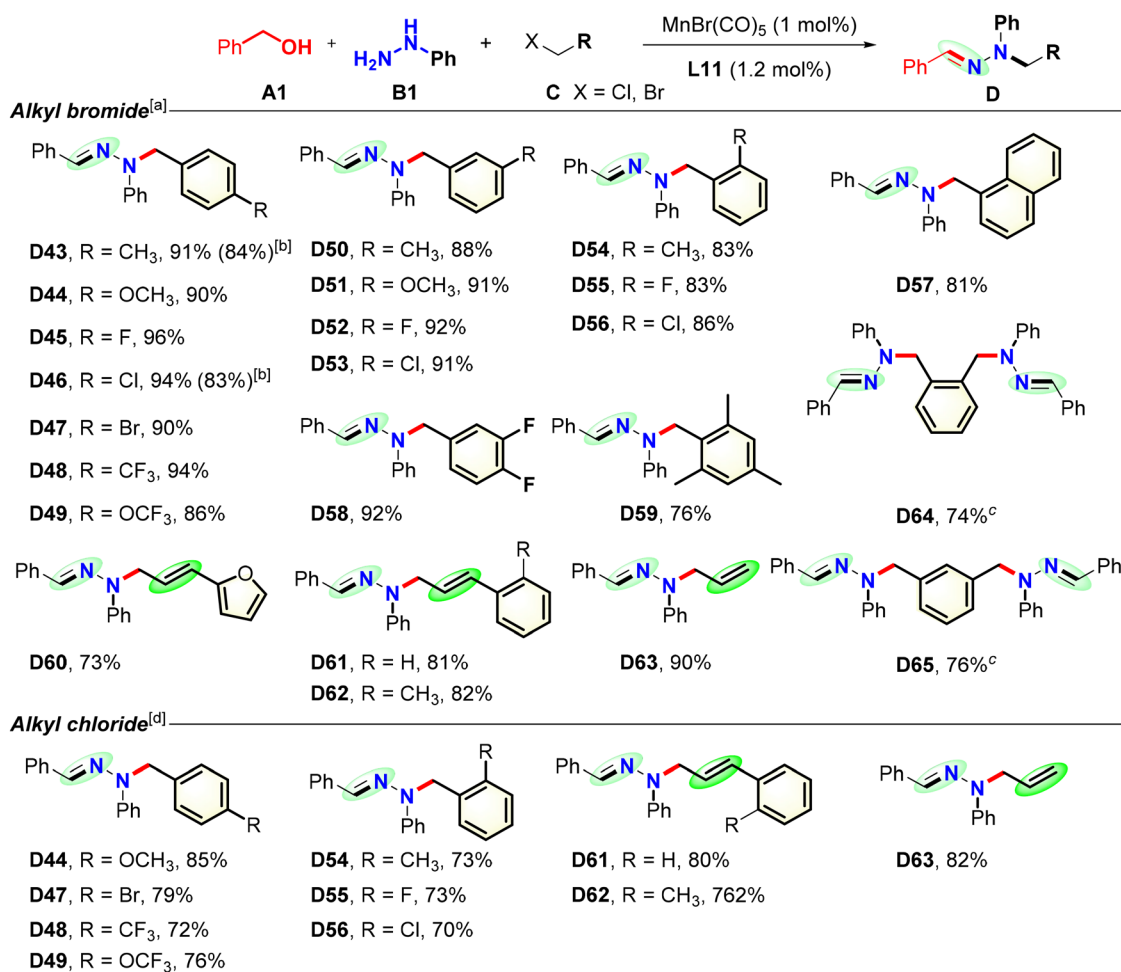
**Scheme 1** Substrate scope of hydrazones derived from various alcohols. <sup>a</sup> Conditions: **A** (0.8 mmol), **B1** (0.5 mmol), **C1** (0.7 mmol), Mn(CO)<sub>5</sub>Br (1.0 mol%), **L11** (1.2 mol%), <sup>t</sup>BuOK (1.0 mmol), THF (3.0 mL), 100 °C, 12 h. Isolated yields. <sup>b</sup> 10 mmol scale, 24 h. <sup>c</sup> <sup>t</sup>BuOK (1.8 mmol).



(D27–D31). Naphthyl, anthryl, and carbazolyl groups are tolerated under the standard catalytic conditions, yielding the desired products D32–D35 in high to excellent yields. To further explore the synthetic potential of this transformation, more challenging aliphatic alcohol substrates were used under the standard reaction conditions. Alkyl alcohols are good dehydrogenation partners, providing D36–D38 in good yields. Alkyl alcohols bearing various types of C=C bonds are also good coupling partners, providing D39–D42 in good to high yields, while the internal double bonds remain intact. The structures of D4 and D26 were confirmed using single-crystal X-ray diffraction.<sup>17</sup> Gram-scale reactions using this Mn catalytic system are successful, producing D2 and D12 in high yields.<sup>16</sup> Disappointingly, secondary alcohols did not work under the standard reaction conditions.

The scope of tandem dehydrogenation condensation with respect to alkyl halide substrates is shown in Scheme 2. A1 and B1 were employed with a series of alkyl halide derivatives, leading to the efficient production of various hydrazones and demonstrating the excellent tolerance of different functional

groups. Generally, the yields obtained using benzyl bromides containing electron-withdrawing groups (D43, D44, and D49) are higher than those obtained using benzyl bromides containing electron-donating groups (D46–D48). Additionally, compared to the results obtained using *para*- and *meta*-substituted substrates, steric hindrance is observed when the *ortho*-position of the benzyl bromide is substituted (D54 and D56). The halide groups, in particular, survive well under the standard reaction conditions, leading to the formation of the corresponding desired products in good to excellent yields, which may be used in further transformations to synthesize complicated molecules. The substitution of F<sub>3</sub>C<sup>-</sup> and F<sub>3</sub>CO<sup>-</sup> has no significant influence on the transformation (D48 and D49), and the naphthyl group is smoothly incorporated into D57, resulting in high yields. Substrates containing two bromide groups are successfully transformed into the corresponding bis-hydrazones D64 and D65 in isolated yields of 74% and 76%, respectively. The allyl and cinnamyl groups also survive the standard procedure, leading to the formation of D60–D63 in high yields, while the internal double bonds remain intact.



**Scheme 2** Substrate scope of hydrazones with respect to halides. <sup>a</sup> Conditions: A1 (0.8 mmol), B1 (0.5 mmol), C (0.7 mmol), Mn(CO)<sub>5</sub>Br (1.0 mol%), L11 (1.2 mol%), <sup>t</sup>BuOK (1.0 mmol), THF (3.0 mL), 100 °C, 12 h. Isolated yields. <sup>b</sup> 10 mmol scale, 24 h. <sup>c</sup> A1 (1.6 mmol), B1 (1.0 mmol), <sup>t</sup>BuOK (2.0 mmol), 36 h. <sup>d</sup> C (0.7 mmol), <sup>t</sup>BuOK (1.5 mmol), 130 °C, 24 h.



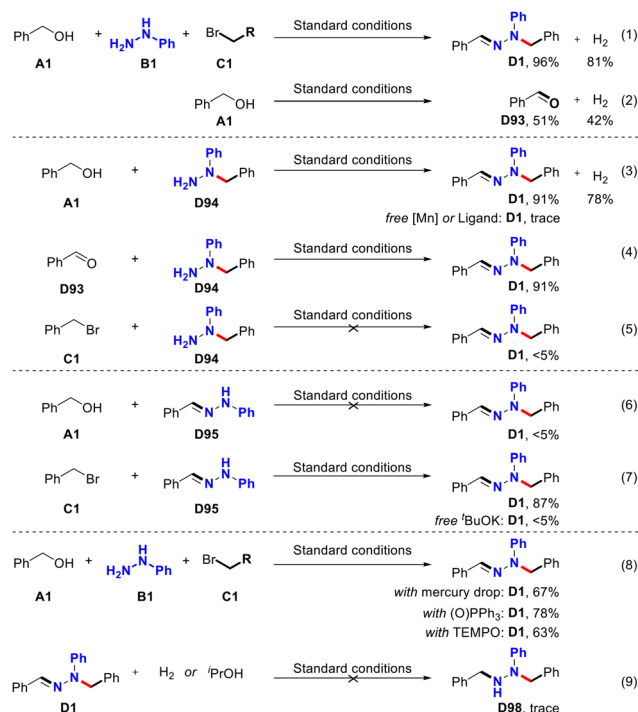
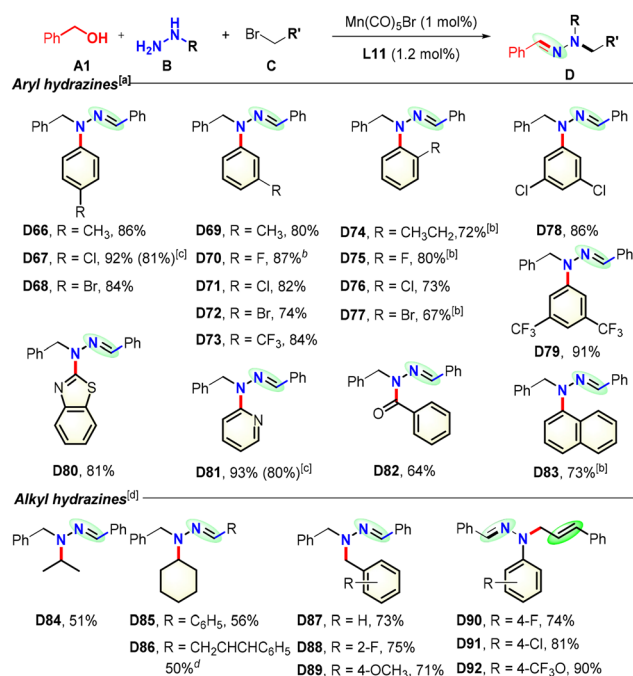


Additionally, the desired hydrazones **D44–D63** are obtained in good to high yields when using more challenging benzyl chloride substrates as reaction partners. Scaled-up reactions (10 mmol scale) proceed easily, furnishing 84% and 83% yields of the hydrazones **D43** and **D46**, respectively.

As tandem dehydrogenative condensation is compatible with a wide range of alkyl halides and alcohols, the scope with respect to the hydrazine was investigated (Scheme 3). With most aromatic hydrazines, the condensation proceeds smoothly to furnish the corresponding desired hydrazones in good to excellent yields. Although numerous hydrazines are in the form of hydrochlorides, hydrazones may be obtained in good to high yields in the presence of 1.5 equivalents of the base. The electronic properties of the phenyl rings of the hydrazines exhibit negligible effects on the reaction. The positions of the substituted functional groups on the phenyl ring clearly influence the efficacy of the transformation, and the corresponding hydrazones (**D74–D77**) are generated in moderate to good yields. Gram-scale reactions are successful, yielding **D67** and **D81** in high amounts.<sup>16</sup> The transformations with halo-substituted hydrazines proceed smoothly to produce the corresponding desired products in 67–92% yields, thus enabling further complex reactions. Additionally, the  $F_3C^-$  group survives well the standard procedure, with the desired adducts **D73** and **D79** formed in good yields, and the naphthyl moieties may be smoothly incorporated into hydrazones. Meanwhile, several heterocyclic moieties, including pyridine

and benzothiazole, are smoothly incorporated into the hydrazone molecules (**D80–D81**) using the corresponding hydrazines. Benzo hydrazide is less reactive with **D82** isolated in a moderate yield. In addition, the desired hydrazone adducts, **D84–D89**, are obtained in moderate to good yields when using more challenging aliphatic hydrazine substrates. These results confirm the viability of the transformation for use in preparing highly functionalized hydrazone derivatives. Furthermore, various allyl halides are compatible with this catalytic dehydrogenation system with various hydrazines, and the desired adducts are isolated in moderate to high yields with excellent regioselectivities (**D90–D92**). Using this tandem dehydrogenation–condensation procedure, gram-scale reactions were successful, yielding **D67** and **D81** in high amounts.<sup>16</sup>

Several mechanistic investigations were performed under the optimal reaction conditions to yield additional data regarding this dehydrogenative condensation, and the results are shown in Fig. 2. Initially,  $H_2$  was analyzed using gas chromatography under the standard conditions, and **D1** could be obtained in an excellent yield, with  $H_2$  detected in 81% yield [eqn (1)], and thus, dehydrogenation may be involved in the catalytic cycle. Additionally, the transformation of **A1** under similar conditions produces **D93** in a moderate yield, and  $H_2$  is detected in 42% yield, with similar results obtained in the presence of a catalytic amount of base [eqn (2)]. These results suggest that (i) dehydrogenation is not only promoted by the Mn catalyst and ligand but also by the catalytic amount of base and (ii) the base may accelerate the condensation process. As 1-benzyl-1-phenylhydrazine (**D94**) is detected when the reaction parameters are optimized, **D94** is employed in



combination with **A1**. A high yield of the desired product **D1** is obtained under the standard conditions, but the reaction shuts down in the absence of the Mn catalyst or ligand, and

**D94** may be recovered in significant quantity. Similar results can be observed in the presence of a catalytic amount of base, and hydrogen is detected in 78% yield [eqn (3)].

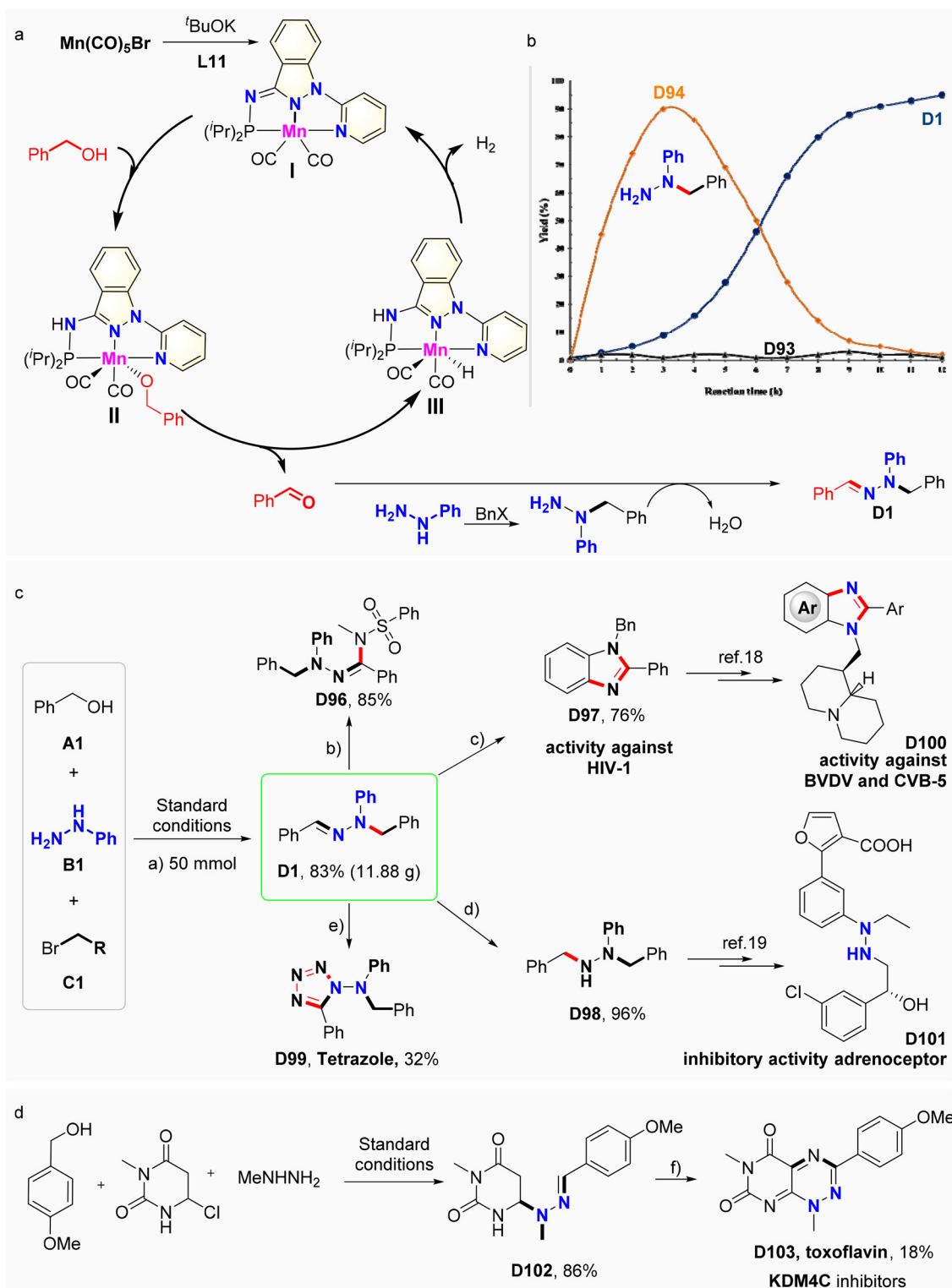


**Fig. 3** Proposed mechanism and possible transformations. (a) Standard conditions. (b) *N*-Methyl-*N*-((phenylsulfonyl)oxy) sulfonamide, Na<sub>2</sub>HPO<sub>4</sub>, *fac*-Ir(ppy)<sub>3</sub>, DCE, 5 W blue light irradiation, 25 °C, 90 h. (c) Cu(OTf)<sub>2</sub>, toluene, 110 °C, 5 h. (d) Pd/C, H<sub>2</sub>, MeOH, 60 °C, 4 h. (e) RVC anode, Pt cathode, TMSN<sub>3</sub>, LiClO<sub>4</sub>, MeCN, MeOH, I (10 mA), 2 h. (f) NaNO<sub>2</sub>, CH<sub>3</sub>COOH, H<sub>2</sub>O, 25 °C, 24 h.



Additionally, **D93** may be employed as a partner for smooth condensation with **D94** in the presence or absence of a catalyst, ligand, or base [eqn (4)]. However, only trace amounts of **D1** are detected with a benzyl bromide partner, and **D98** is obtained in a high yield [eqn (5)]. Hence, (i) **D94** (*in situ*-generated) may be the intermediate because its transformation to **D1** is distinctly observed in the time conversion plot (Fig. 3b); (ii) additives are unnecessary for the condensation process; and (iii) benzyl bromide does not condense under the standard conditions but undergoes nucleophilic substitution in the presence of a base. Furthermore, only trace amounts of **D1** are detected with 1-benzylidene-2-phenylhydrazine (**D95**) as the coupling partner, and H<sub>2</sub> is detected in a moderate yield. This is attributed to the lower nucleophilic attack activity of the NH condensation site of **D95** towards an aldehyde group, and dehydrogenation is unaffected [eqn (6)]. Notably, benzyl bromide as a substrate reacts with **D95**, generating 87% yield of **D1**. **D1** is obtained in a high yield in the absence of a Mn catalyst or a ligand, but the reaction stops in the absence of a base [eqn (7)]. Thus, (i) **D95** could be the intermediate, as its transformation to **D1** is undetected in the time conversion plot (Fig. 3b); (ii) a base is necessary for nucleophilic substitution; and (iii) **A1** is involved in the hydrazone backbone that should undergo dehydrogenation.

Additionally, a Hg drop experiment was performed, resulting in acceptable yields of the desired product **D1** without causing a significant decrease in yields. These results demonstrate the significant role of the Mn catalyst in promoting the dehydrogenative reaction. Thereafter, TEMPO was added as the radical scavenger under the standard conditions, and **D1** was obtained in good yield, suggesting that this dehydrogenation could not be a free radical process [eqn (8)]. The time conversion plot reveals that the concentration of the intermediate **D94** initially increases and then decreases with increasing reaction time. The concentration of **D93** is maintained at trace levels, indicating that the condensation of the aldehyde with **D94** is relatively rapid. These results further confirm that the formation of the intermediate **D94** and the dehydrogenation are the rate-determining steps in the transformation reaction. Furthermore, only a trace amount of the product **D98** was obtained when using **D1** as the partner in the presence of H<sub>2</sub> or <sup>1</sup>PrOH as the solvent under the standard conditions [eqn (9)]. These results show that the catalytic system is not sufficiently active for the catalytic reductive hydrogenation of ylidenehydrazines.

Although the precise mechanism remains unclear, a possible mechanism of the tandem dehydrogenation condensation is shown in Fig. 3a. Initially, the Mn species **I** is produced from Mn(CO)<sub>5</sub>Br and **L11** in the presence of a base under catalytic reaction conditions. The oxidative addition of the alcohol to **I** generates the key alkoxy-Mn species **II**. The putative Mn species **III** may be generated *via* β-hydrogen elimination and release the aldehyde. Subsequent reductive elimination releases **I** and H<sub>2</sub>. Thereafter, **I** is re-oxidized to regenerate the active Mn catalyst for use in the next catalytic cycle. Aldehyde condensation with *in situ*-generated **D94** from hydrazine and

benzyl bromide produces the desired product. Another pathway involves the direct condensation of the aldehyde with hydrazine to produce **D95**, which yields the product *via* nucleophilic substitution with benzyl bromide in the presence of a base.

To further demonstrate the robustness of the tandem dehydrogenation condensation reaction, we conducted a reaction on a gram scale to produce **D1** in a high yield (11.88 g) (Fig. 3).<sup>16</sup> Ylidenehydrazines are attractive reactive building blocks that may be readily utilized in synthesizing functionalized complex products (Fig. 3c). **D1** may be easily converted to functional nitrogenous heterocyclic compounds, such as benzimidazole (**D97**) and tetrazole (**D99**), *via* cyclization reactions. **D98** is obtained in an excellent yield *via* reductive conversion; furthermore, a high yield of **D96** is obtained *via* sulfonamidation. The CVB-5 pharmaceutical (**D100**) could be synthesis from **D97**.<sup>18</sup> Furthermore, **D98** could be produced into the desired inhibitory activity adrenoceptor pharmaceutical (**D101**).<sup>19</sup> Additionally, with the newly developed catalytic system, the desired product (**D102**) was isolated in 86% yield, which could be transformed into the KDM4C inhibitor pharmaceutical toxoflavin (**D103**) in an acceptable isolated yield (Fig. 3d).<sup>20</sup>

## Conclusions

In summary, we have initiated the unprecedented transition metal Mn-catalyzed tandem dehydrogenative condensation coupling of hydrazines with alcohols and halides to generate trisubstituted hydrazones, overcoming the challenge of selectivity in multicomponent reactions. Based on the complexation of the Earth-abundant Mn with a readily available PNN pincer ligand, this catalytic system not only provides an efficient method for preparing gram-scale (11.88 g) hydrazones but also facilitates the preparation of various novel hydrazone derivatives. Using this protocol, several pharmaceuticals may be easily synthesized. These are the first direct one-pot syntheses of hydrazones *via* dehydrogenation, liberating H<sub>2</sub>. This strategy significantly broadens the scope of Mn-catalyzed dehydrogenative condensation coupling for synthesizing unsaturated molecules. Studies aimed at obtaining a detailed mechanistic understanding of these tandem dehydrogenative condensation coupling reactions and the application of this strategy in other transformations are currently ongoing.

## Conflicts of interest

The authors declare no conflict of interest.

## Acknowledgements

This work was supported by the National Natural Science Foundation of China (22002067 and 22202228), the Hundred-Talent Program of the Chinese Academy of Sciences, the Fund



Program for the Scientific Activities of Selected Returned Overseas Professionals in Shanxi Province (20220052), the Science and Technology Project of Shanxi Province (202103021223457), and the State Key Laboratory of Coal Conversion, Institute of Coal Chemistry, Chinese Academy of Sciences (2021BWZ011).

## References

- (a) A. Raja, J. Lebbos and P. Kirkpatrick, Atazanavir sulphate, *Nat. Rev. Drug Discovery*, 2003, **2**, 857–858; (b) R. Chingle, C. Proulx and W. D. Lubell, Azapeptide synthesis methods for expanding sidechain diversity for biomedical applications, *Acc. Chem. Res.*, 2017, **50**, 1541–1556; (c) Z. Ko-kan and M. J. Chmielewski, A photoswitchable heteroditopic ion-pair receptor, *J. Am. Chem. Soc.*, 2018, **140**, 16010–16014; (d) M. Li, L. P. Cheng, W. Pang, Z. J. Zhong and L. L. Guo, Design, synthesis, and biological evaluation of novel acylhydrazone derivatives as potent neuraminidase inhibitors, *ACS Med. Chem. Lett.*, 2020, **11**, 1745–1750; (e) G. Bagnolini, B. Balboni, F. Schipani, D. Gioia, M. Veronesi, F. D. Franco, C. Kaya, R. P. Jumde, J. A. Ortega, S. Giroto, A. K. H. Hirsch, M. Roberti and A. Cavalli, Identification of RAD51–BRCA2 inhibitors using N-acylhydrazone-based dynamic combinatorial chemistry, *ACS Med. Chem. Lett.*, 2022, **13**, 1262–1269.
- (a) J. W. Cahn and R. E. Powell, The Raschig synthesis of hydrazine, *J. Am. Chem. Soc.*, 1954, **76**, 2565–2567; (b) B. M. Trost and M. L. Crawley, Asymmetric transition-metal-catalyzed allylic alkylations: applications in total synthesis, *Chem. Rev.*, 2003, **103**, 2921–2944; (c) M. Kilian and N. Martin, Catalytic activation of N–N multiple bonds: a homogeneous palladium catalyst for mechanistically unprecedented reduction of azo compounds, *Angew. Chem., Int. Ed.*, 2006, **45**, 2305–2308; (d) S. Shirakawa, P. J. Lombard and J. L. Leighton, A simple and general chiral silicon lewis acid for asymmetric synthesis: highly enantioselective [3 + 2] acylhydrazone-enol ether cycloadditions, *J. Am. Chem. Soc.*, 2015, **127**, 9974–9975; (e) A. J. Waldman, T. L. Ng, P. Wang and E. P. Balskus, Heteroatom–heteroatom bond formation in natural product biosynthesis, *Chem. Rev.*, 2017, **117**, 5784–5863; (f) S. Shahi, H. Roghani-Mamaqani, R. Hoogenboom, S. Talebi and H. Mardani, Stimuli-responsive covalent adaptable hydrogels based on homolytic bond dissociation and chain transfer reactions, *Chem. Mater.*, 2022, **34**, 468–498.
- (a) J. G. De Vries and C. J. Elsevier, *The handbook of homogeneous hydrogenation*, Wiley-VCH, Weinheim, 2007; (b) J. F. Sonnenberg, N. Coombs, P. A. Dube and R. H. Morris, Iron nanoparticles catalyzing the asymmetric transfer hydrogenation of ketones, *J. Am. Chem. Soc.*, 2012, **134**, 5893–5899.
- (a) F. Li, C. Sun and N. Wang, Catalytic acceptorless dehydrogenative coupling of arylhydrazines and alcohols for the synthesis of arylhydrazones, *J. Org. Chem.*, 2014, **79**, 8031–8039; (b) L. Hao, G. Wang, J. Sun, J. Xu, H. Li, G. Duan, C. Xia and P. Zhang, From phenylhydrazone to 1H-1,2,4-triazoles via nitrication, reduction and cyclization, *Adv. Synth. Catal.*, 2020, **362**, 1657–1662.
- (a) M. J. Hülsey, H. Yang and N. Yan, Sustainable routes for the synthesis of renewable heteroatom-containing chemicals, *ACS Sustainable Chem. Eng.*, 2018, **6**, 5694–5707; (b) S. Michlik and R. Kempe, A sustainable catalytic pyrrole synthesis, *Nat. Chem.*, 2013, **5**, 140–144; (c) K. Weissermel and H.-J. Arpe, *Industrial organic chemistry*, Wiley-VCH, Weinheim, 2003.
- (a) A. Kumar, P. Daw and D. Milstein, Homogeneous catalysis for sustainable energy: hydrogen and methanol economies, fuels from biomass, and related topics, *Chem. Rev.*, 2022, **122**, 385–441; (b) K. Barta and P. C. Ford, Catalytic conversion of nonfood woody biomass solids to organic liquids, *Acc. Chem. Res.*, 2014, **47**, 1503–1512; (c) T. P. Vispute, H. Zhang, A. Sanna, R. Xiao and G. W. Huber, Renewable chemical commodity feedstocks from integrated catalytic processing of pyrolysis oils, *Science*, 2010, **330**, 1222–1227.
- (a) R. H. Crabtree, Deactivation in homogeneous transition metal catalysis: causes, avoidance, and cure, *Chem. Rev.*, 2015, **115**, 127–150; (b) F. Kallmeier, T. Irrgang, T. Dietel and R. Kempe, Highly active and selective manganese C=O bond hydrogenation catalysts: the importance of the multi-dentate ligand, the ancillary ligands, and the oxidation state, *Angew. Chem., Int. Ed.*, 2016, **55**, 11806–11809; (c) S. Elangovan, C. Topf, S. Fischer, H. Jiao, A. Spannenberg, W. Baumann, R. Ludwig, K. Junge and M. Beller, Selective catalytic hydrogenations of nitriles, ketones, and aldehydes by well-defined manganese pincer complexes, *J. Am. Chem. Soc.*, 2016, **138**, 8809–8814; (d) M. Garbe, K. Junge, S. Walker, Z. Wei, H. Jiao, A. Spannenberg, S. Bachmann, M. Scalone and M. Beller, Manganese(I)-catalyzed enantioselective hydrogenation of ketones using a defined chiral PNP pincer ligand, *Angew. Chem., Int. Ed.*, 2017, **56**, 11237–11241; (e) M. B. Widegren, G. J. Harkness, A. M. Z. Slawin, D. B. Cordes and M. L. Clarke, A highly active manganese catalyst for enantioselective ketone and ester hydrogenation, *Angew. Chem., Int. Ed.*, 2017, **56**, 5825–5828.
- (a) G. Guillena, D. J. Ramon and M. Yus, Hydrogen auto-transfer in the N-alkylation of amines and related compounds using alcohols and amines as electrophiles, *Chem. Rev.*, 2010, **110**, 1611–1641; (b) J. Choi, A. H. MacArthur, M. Brookhart and A. S. Goldman, Dehydrogenation and related reactions catalyzed by iridium pincer complexes, *Chem. Rev.*, 2011, **111**, 1761–1779; (c) Y. Obora, Recent advances in  $\alpha$ -alkylation reactions using alcohols with hydrogen borrowing methodologies, *ACS Catal.*, 2014, **4**, 3972–3981; (d) Q. Yang, Q. Wang and Z. Yu, Substitution of alcohols by N-nucleophiles via transition metal-catalyzed





- dehydrogenation, *Chem. Soc. Rev.*, 2015, **44**, 2305–2329; (e) A. Quintard and J. Rodriguez, A step into an eco-compatible future: iron- and cobalt-catalyzed borrowing hydrogen transformation, *ChemSusChem*, 2016, **9**, 28–30; (f) Y. Xie, Y. Ben-David, L. J. W. Shimon and D. Milstein, Highly efficient process for production of biofuel from ethanol catalyzed by ruthenium pincer complexes, *J. Am. Chem. Soc.*, 2016, **138**, 9077–9080; (g) S. Lv, X. Han, J.-Y. Wang, M. Zhou, Y. Wu, L. Ma, L. Niu, W. Gao, J. Zhou, W. Hu, Y. Cui and J. Chen, *Angew. Chem., Int. Ed.*, 2020, **59**, 11583–11590; (h) P. Zhang, B. Li, L. Niu, L. Wang, G. Zhang, X. Jia, G. Zhang, S. Liu, L. Ma, W. Gao, D. Qin and J. Chen, Scalable Electrochemical Transition-Metal-Free Dehydrogenative Cross-Coupling Amination Enabled Alkaloid Clausines Synthesis, *Adv. Synth. Catal.*, 2020, **362**, 2342–2347.
- 9 (a) C. O. Tuck, E. Perez, I. T. Horvath, R. A. Sheldon and M. Poliakoff, Valorization of biomass: deriving more value from waste, *Science*, 2012, **337**, 695–699; (b) W. Zuo, A. J. Lough, Y. F. Li and R. H. Morris, Amine(imine)diphosphine iron catalysts for asymmetric transfer hydrogenation of ketones and imines, *Science*, 2013, **342**, 1080–1083; (c) G. Zhang, K. V. Vasudevan, B. L. Scott and S. K. Hanson, Understanding the mechanisms of cobalt-catalyzed hydrogenation and dehydrogenation reactions, *J. Am. Chem. Soc.*, 2013, **135**, 8668–8681; (d) C. Gunanathan and D. Milstein, Applications of acceptorless dehydrogenation and related transformations in chemical synthesis, *Science*, 2013, **341**, 1229712; (e) S. Fleischer, S. Zhou, K. Junge and M. Beller, General and highly efficient iron-catalyzed hydrogenation of aldehydes, ketones, and  $\alpha$ ,  $\beta$ -unsaturated aldehydes, *Angew. Chem., Int. Ed.*, 2013, **52**, 5120–5124; (f) T. Yan, B. L. Feringa and K. Barta, Iron catalysed direct alkylation of amines with alcohols, *Nat. Commun.*, 2014, **5**, 5602; (g) S. Qu, Y. Dang, C. Song, M. Wen, K.-W. Huang and Z.-X. Wang, Catalytic mechanisms of direct pyrrole synthesis via dehydrogenative coupling mediated by PNP-Ir or PNN-Ru pincer complexes: crucial role of proton-transfer shuttles in the PNP-Ir system, *J. Am. Chem. Soc.*, 2014, **136**, 4974–4991; (h) S. Chakraborty, H. Dai, P. Bhattacharya, N. T. Fairweather, M. S. Gibson, J. A. Krause and H. Guan, Iron-based catalysts for the hydrogenation of esters to alcohols, *J. Am. Chem. Soc.*, 2014, **136**, 7869–7872; (i) D. Gärtner, A. Welther, B. R. Rad, R. Wolf and A. J. von Wangelin, Heteroatom-free arene-cobalt and arene-iron catalysts for hydrogenations, *Angew. Chem., Int. Ed.*, 2014, **53**, 3722–3726; (j) T. J. Korstanje, J. Ivar van der Vlugt, C. J. Elsevier and B. de Bruin, Hydrogenation of carboxylic acids with a homogeneous cobalt catalyst, *Science*, 2015, **350**, 298–302; (k) N. Deibl and R. Kempe, General and mild cobalt-catalyzed C-alkylation of unactivated amides and esters with alcohols, *J. Am. Chem. Soc.*, 2016, **138**, 10786–10789; (l) L. De Luca and A. Mezzetti, Base-free asymmetric transfer hydrogenation of 1,2-di- and monoketones catalyzed by a  $(\text{NH})_2\text{P}_2$ -macrocylic iron(II) hydride, *Angew. Chem., Int. Ed.*, 2017, **56**, 11949–11953; (m) W. Yang, I. Yu. Chernyshov, M. Weber, E. A. Pidko and G. A. Filonenko, Switching between hydrogenation and olefin transposition catalysis via Silencing NH cooperativity in Mn(I) pincer complexes, *ACS Catal.*, 2022, **12**, 10818–10825; (n) Y. F. Gu, T. Y. Wang, M. Gao and Z. J. Yao, Scalable Cu(II)-mediated intramolecular dehydrogenative phenol-phenol coupling: Concise synthesis of enantiopure axially chiral homo- and hetero-diphenols, *Chin. Chem. Lett.*, 2021, **32**, 380–384.
- 10 (a) S. Elangovan, M. Garbe, H. Jiao, A. Spannenberg, K. Junge and M. Beller, Hydrogenation of esters to alcohols catalyzed by defined manganese pincer complexes, *Angew. Chem., Int. Ed.*, 2016, **55**, 15364–15368; (b) M. Mastalir, M. Glatz, E. Pittenauer, G. Allmaier and K. Kirchner, Sustainable synthesis of quinolines and pyrimidines catalyzed by manganese PNP pincer complexes, *J. Am. Chem. Soc.*, 2016, **138**, 15543–15546; (c) D. Milstein, A. Kumar, N.-A. Espinosa-Jalapa, G. Leitus, Y. Diskin-Posner and L. Avram, Direct synthesis of amides by dehydrogenative coupling of amines with either alcohols or esters: manganese pincer complex as catalyst, *Angew. Chem., Int. Ed.*, 2017, **56**, 14992–14996; (d) S. Chakraborty, U. K. Das, Y. Ben-David and D. Milstein, Manganese catalyzed  $\alpha$ -olefination of nitriles by primary alcohols, *J. Am. Chem. Soc.*, 2017, **139**, 11710–11713; (e) A. Zirakzadeh, S. R. M. M. de Aguiar, B. Stöger, M. Widhalm and K. Kirchner, Enantioselective transfer hydrogenation of ketones catalyzed by a manganese complex containing an unsymmetrical chiral PNP' tridentate ligand, *ChemCatChem*, 2017, **9**, 1744–1748; (f) A. Dubey, L. Nencini, R. R. Fayzullin, C. Nervi and J. R. Khusnutdinova, Bio-inspired Mn(I) complexes for the hydrogenation of  $\text{CO}_2$  to formate and formamide, *ACS Catal.*, 2017, **7**, 3864–3868; (g) A. Bruneau-Voisine, D. Wang, V. Dorcet, T. Roisnel, C. Darcel and J.-B. Sortais, Transfer hydrogenation of carbonyl derivatives catalyzed by an inexpensive phosphinefree manganese precatalyst, *Org. Lett.*, 2017, **19**, 3656–3659; (h) O. Martínez-Ferraté, C. Werlé, G. Franciò and W. Leitner, Aminotriazole Mn(I) complexes as effective catalysts for transfer hydrogenation of ketones, *ChemCatChem*, 2018, **10**, 4514–4518; (i) K. Ganguli, S. Shee, D. Panjaa and S. Kundu, Cooperative Mn(I)-complex catalyzed transfer hydrogenation of ketones and imines, *Dalton Trans.*, 2019, **48**, 7358–7366; (j) N. V. Shvydkiy, O. Vyshivskiy, Y. V. Nelyubina and D. S. Perekalin, Design of manganese phenol pi-complexes as shvo-type catalysts for transfer hydrogenation of ketones, *ChemCatChem*, 2019, **11**, 1602–1605; (k) S. Waiba, M. Maiti and B. Maji, Manganese-catalyzed reformation of vicinal glycols to  $\alpha$ -hydroxy carboxylic acids with the liberation of hydrogen gas, *ACS Catal.*, 2022, **12**, 3995–4001; (l) Q. Liang, C. Zhang, F. Wang, Z. Luo, W. Yang, G. Zhang, D. Ding and G. Zhang, Triazole backbone ligand in an unprecedented efficient manganese catalyst for use in transfer hydrogenation, *Sci. China: Chem.*, 2023, **66**, 2028–2036.
- 11 (a) Y. Zhou, X. Shan, R. Mas-Balleste, M. R. Bukowski, A. Stubna, M. Chakrabarti, L. Slominski, J. A. Halfen,



- E. Muenck and Q. Lawrence Jr., Contrasting cis and trans effects on the reactivity of nonheme oxoiron(IV) complexes, *Angew. Chem., Int. Ed.*, 2008, **47**, 1896–1899; (b) B. Tu, Q. Pang, H. Xu, X. Li, Y. Wang, Z. Ma, L. Weng and Q. Li, Reversible redox activity in multicomponent meta-organic frameworks constructed from trinuclear copper pyrazolate building blocks, *J. Am. Chem. Soc.*, 2017, **139**, 7998–8007; (c) K. Warm, G. Tripodi, E. Andris, S. Mebs, U. Kuhlmann, H. Dau, P. Hildebrandt, J. Roithová and K. Ray, Spectroscopic characterization of a reactive  $[\text{Cu}_2(\mu\text{-OH})_2]^{2+}$  intermediate in Cu/TEMPO catalyzed aerobic alcohol oxidation reaction, *Angew. Chem., Int. Ed.*, 2021, **60**, 23018–23024.
- 12 (a) Y. Wang, D. Zhu, L. Tang, S. Wang and Z. Wang, Highly efficient amide synthesis from alcohols and amines by virtue of a water-soluble gold/DNA catalyst, *Angew. Chem., Int. Ed.*, 2011, **50**, 8917–8921; (b) M. Tamura and K. Tomishige, Redox properties of  $\text{CeO}_2$  at low temperature: the direct synthesis of imines from alcohol and amine, *Angew. Chem., Int. Ed.*, 2015, **54**, 864–867; (c) C. Zhang, Q. Liang, W. Yang, G. Zhang, M. Hu and G. Zhang, Nickel (I)-catalyzed (de)hydrogenative coupling of amines and alkyl heteroarenes with alcohols, *Green Chem.*, 2022, **24**, 7368–7375.
- 13 G. Zhang, T. Irrgang, M. Schlagbauer and R. Kempe, Synthesis of 1,3-diketones from esters via liberation of hydrogen, *Chem. Catal.*, 2021, **1**, 681–690.
- 14 (a) N. Deibl and R. Kempe, Manganese-Catalyzed Multicomponent Synthesis of Pyrimidines from Alcohols and Amines, *Angew. Chem., Int. Ed.*, 2017, **56**, 1663–1666; (b) G. Zhang, T. Irrgang, T. Dietel, F. Kallmeier and R. Kempe, Manganese-catalyzed dehydrogenative alkylation or  $\alpha$ -olefination of alkyl-substituted N-heteroarenes with alcohols, *Angew. Chem., Int. Ed.*, 2018, **57**, 9131–9135.
- 15 (a) E. Balaraman, E. Khaskin, G. Leitus and D. Milstein, Catalytic transformation of alcohols to carboxylic acid salts and  $\text{H}_2$  using water as the oxygen atom source, *Nat. Chem.*, 2013, **5**, 122–125; (b) S. Elangovan, J. Neumann, J.-B. Sortais, K. Junge, C. Darcel and M. Beller, Efficient and selective N-alkylation of amines with alcohols catalysed by manganese pincer complexes, *Nat. Commun.*, 2016, **7**, 12641; (c) M. Perez, S. Elangovan, A. Spannenberg, K. Junge and M. Beller, Molecularly defined manganese pincer complexes for selective transfer hydrogenation of ketones, *ChemSusChem*, 2017, **10**, 83–86; (d) M. Mastalir, E. Pittenauer, G. Allmaier and K. Kirchner, Manganese-catalyzed aminomethylation of aromatic compounds with methanol as a sustainable C1 building block, *J. Am. Chem. Soc.*, 2017, **139**, 8812–8815; (e) G. A. Filonenko, R. van Putten, E. J. M. Hensen and E. A. Pidko, Catalytic (de)hydrogenation promoted by non-precious metals – Co, Fe and Mn: recent advances in an emerging field, *Chem. Soc. Rev.*, 2018, **47**, 1459–1483; (f) Y. Wang, M. Wang, Y. Li and Q. Liu, Homogeneous manganese-catalyzed hydrogenation and dehydrogenation reactions, *Chem*, 2021, **7**, 1180–1223; (g) A. E. Owen, A. Preiss, A. McLuskie, C. Gao, G. Peters, M. Bühl and A. Kumar, Manganese-catalyzed dehydrogenative synthesis of urea derivatives and polyureas, *ACS Catal.*, 2022, **12**, 6923–6933.
- 16 See the ESI† for details.
- 17 **D4** (CCDC 2288831), **D26** (CCDC 2288839).†
- 18 (a) M. Tonelli, F. Novelli, B. Tasso, I. Vazzana, A. Sparatore, V. Boido, F. Sparatore, P. L. Colla, G. Sanna, G. Giliberti, B. Busonera, P. Farci, C. Ibba and R. Loddo, Antiviral activity of benzimidazole derivatives. III. novel anti-CVB-5, anti-RSV and anti-Sb-1 agents, *Bioorg. Med. Chem.*, 2014, **22**, 4893–4909; (b) V. Boido, G. Paglietti, M. Tonelli and G. Vitale, Nonnucleoside benzimidazoles as antiviral drugs against HIV infections, in *RNA-Viruses. Enzymatic and Receptor Inhibitors*, ed. A. Carta, Research Signpost, Kerala, 2009, pp. 1–39.
- 19 C. H. Boehringer, Sohn AG & Co., KG-US2009/12161, A9, 2009.
- 20 (a) J. Zeller, A. J. Turbiak, I. A. Powelson, S. Lee, D. Sun, H. D. Hollis Showalter and E. R. Fearon, Investigation of 3-aryl-pyrimido[5,4-e] [1,2,4] triazine-5,7-diones as small molecule antagonists of  $\beta$ -catenin/TCF transcription, *Bioorg. Med. Chem.*, 2013, **23**, 5814–5820; (b) V. Letfus, D. Jelić, A. Bokulić, A. Petrinić Grba and S. Koštrun, Rational design, synthesis and biological profiling of new KDM4C inhibitors, *Bioorg. Med. Chem.*, 2020, **28**, 115128.

